PHYSICAL REVIEW VOLUME 108, NUMBER 5 DECEMBER 1, 1957

Nuclear Magnetic Resonance in Paramagnetic MnF_2

R. G. SHULMAN AND V. JACCARINO
Bell Telephone Laboratories, Murray Hill, New Jersey

(Received May 8, 1957)

Nuclear magnetic resonances of F^{19} in single crystals of paramagnetic MnF_2 have been observed in the temperature region 68°K to 300°K. Shifts of the resonances from the predicted field, ω/γ, were as large as eight percent. With the external magnetic field not in the *ab* plane, two separate resonances were observed corresponding to the two different fluorine positions in the unit cell. Both the shifts and the splittings were functions of magnetic field, temperature, and crystal orientation. As the temperature was increased, the line widths increased from 25 to 42 oe. These observations were explained by postulating a small degree of covalency in the F^- bond to the paramagnetic Mn^{++} ion. Each bond includes $0.48\pm0.02\%$ fluorine $2s$ character. The contributions of the $2p_\sigma$ and $2p_\pi$ orbitals are discussed and the effects of the covalency upon the long-range order and the superexchange mechanism are considered.

The lines disappeared abruptly at the Néel temperature, T_n, (68 ± 1°K) because the sudden increase in sublattice magnetization shifts them beyond the frequency range of the spectrometer. Attempts to observe the resonances at low temperatures are described.

INTRODUCTION

BLOEMBERGEN[1] first drew attention to the importance of nuclear magnetic resonance (NMR) studies of nuclei of nonmagnetic atoms in paramagnetic crystals. Large internal dipole fields arising from the electronic spins are characteristic of paramagnetic substances. In the absence of line-narrowing mechanisms the NMR is broadened by these dipole fields and would, in general, be unobservable. However, if rapid electronic motions, such as may result from exchange interactions, exist in the solid, the NMR may be "exchange narrowed."[2] In addition to these narrowing effects, the strong exchange interactions may lead to an ordered state at low temperatures. (For example, MnF_2 is antiferromagnetic below 68°K.)

In the paramagnetic state the NMR would be expected to be displaced from its normal field of ω/γ_N by the time-averaged field, at the nuclear positions, from the magnetic ions. The magnitude of this field is $\mu(\mu H_0/kT)(1/a^3)$, where μ is the electronic moment, H_0 the external magnetic field and a is the interatomic spacing. It can be seen to be of the order of several oersteds for $\mu=g\beta$, $H_0=5000$ oe, $T=100$°K, and $a=2$ A. For nonequivalent nuclear positions in the unit magnetic cell the different displacements result in small splittings of the NMR which will vary with the angle between the external magnetic field and the crystalline axes. Line breadths and the nuclear spin-lattice relaxation time would be determined by the aforementioned "exchange narrowing," the frequency breadth being of the order $\omega\cong\omega_d^2/\omega_e$, where ω_d is the dipolar frequency breadth expected in the absence of exchange forces and $\omega_e=J/\hbar$, where J is the exchange energy.

In the ordered state the NMR would be displaced by local fields of the order of $(\mu/a^3)[M(T)/M(0)]$, where $M(T)$ is the sublattice magnetization at temperature T. In the molecular field theory of antiferromagnetism $M(T)/M(0)$ is the normalized Brillouin function which is unity at $T=0$ and vanishes at the transition temperature. Owing to the antiparallel ordering and the relative proximity of nuclei to a spin of a given orientation an additional splitting will, in general, occur. Indeed, it was just this effect which led Poulis *et al.*[3] to the discovery of antiferromagnetism in $CuCl_2\cdot 2H_2O$ while observing the proton resonance as a function of temperature. The shift of the NMR line will therefore be a measure of the magnitude and temperature dependence of the sublattice magnetization. In the antiferromagnetic state the NMR line width and nuclear spin-lattice relaxation time will be functions of the collective motions of the electronic spins. At temperatures small compared to the transition temperature, the dominant relaxation mechanism is the inelastic scattering of spin waves by the nuclear magnetic moments. The applicability of spin-wave theory to this problem has been the subject of two recent papers.[4,5] The experimental determination in MnF_2 of the magnitude and temperature dependence of T_1 and T_2 would provide an interesting comparison with theory.

These qualitative comments summarize the results observed in the only two stoichiometric paramagnetics previously studied ($CuSO_4\cdot 5H_2O$ and $CuCl_2\cdot 2H_2O$). In these cases the NMR lines observed were from the protons in the water of hydration. The protons may be thought of as noninteracting field probes in these compounds. If, however, one looks at the nuclear magnetic resonance of the nuclei of those nonmagnetic ions which are bonded to the paramagnetic ions [e.g., F^{19} in MnF_2, $Cl^{35,37}$ in $CuCl_2\cdot 2H_2O$], the effects of electron transfer will, as we shall see, cause relatively enormous shifts and splittings in the paramagnetic

---

[1] N. Bloembergen, Physica **16**, 95 (1950); N. Bloembergen and N. J. Poulis, Physica **16**, 915 (1950).

[2] P. W. Anderson and P. R. Weiss, Revs. Modern Phys. **25**, 269 (1953).

[3] Poulis, Hardeman, and Bölger, Physica **18**, 429 (1952).

[4] J. Van Kranendonk and M. Bloom, Physica **22**, 545 (1956).

[5] T. Moriya, Progr. Theoret. Phys. Japan **16**, 23 (1956).

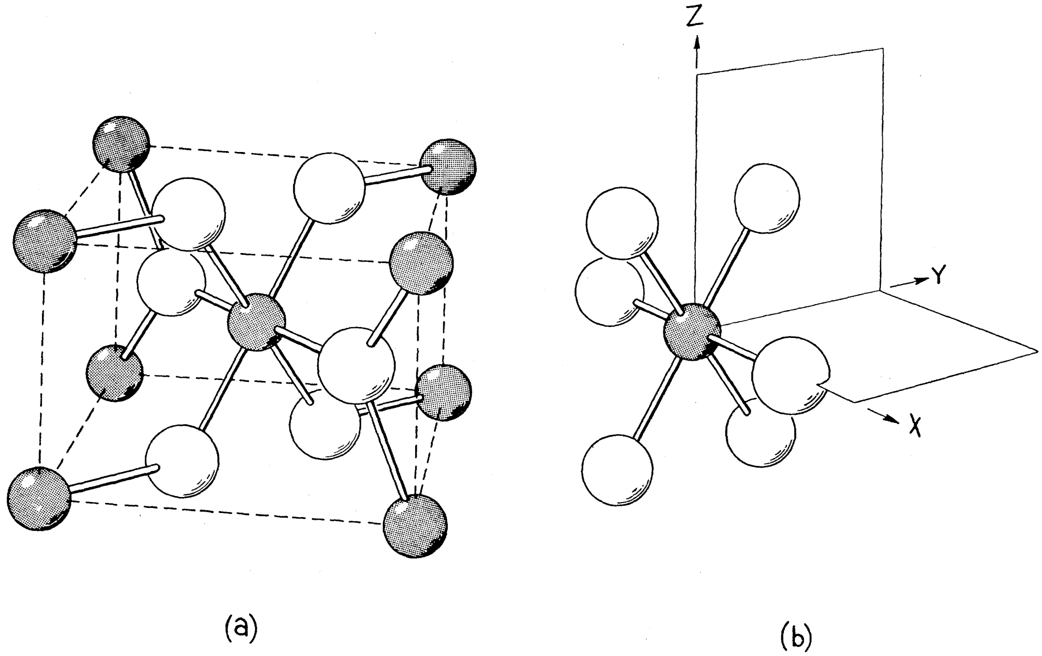

FIG. 1. (a) Unit cell of MnF$_2$. Neutron diffraction data indicate that the corner and body-centered Mn^{++} ions are oppositely directed, parallel to the c axis. (The chemical and magnetic unit cells are the same.) (b) A perspective of a Mn^{++} ion and the distorted octahedral of F$^-$ ions that surround it. We note that c axis, [001], and z direction are used interchangeably here and in the text. A similar interchange of nomenclature for the other important crystalline directions is used as well.

state, and, in the antiferromagnetic state, will result in a very high-frequency nuclear magnetic resonance even in the absence of an external magnetic field.

MnF$_2$, manganous fluoride, has the rutile structure[6] with tetragonal symmetry. The unit cell contains two cations and four anions; the basic structure is given in Fig. 1(a). In the antiferromagnetic state the Mn^{++} ions are ordered so as to consist of two interpenetrating sublattices with oppositely oriented spins. With respect to a given Mn^{++} ion the two nearest neighbors along the tetragonal axis are ferromagnetically aligned and the eight next nearest neighbors along body diagonals are antiferromagnetically aligned. The local symmetry of each Mn^{++} is, however, only orthorhombic, with the other cation in the unit cell having its axes differing by a 90° rotation about the c axis designated by [001]. There are two distinguishable fluorine positions in the unit cell lying in (110) and $(\bar{1}10)$ planes, respectively. Because of the 90° rotation the two fluorine sites are interchanged in going from one Mn^{++} to the next in the unit cell. The angles between the Mn^{++}—F$^-$—Mn^{++} directions are 102° and 129°. The Mn^{++} has four F$^-$ ions at 2.11 A and two F$^-$ at 2.14 A. Tinkham,[7] whose nomenclature we follow, has, in his discussion of the paramagnetic resonance of Mn^{++} in ZnF$_2$ called the four identical F$^-$ ions type I fluorines and the other two F$^-$ type II. For our purposes the important Mn^{++}—F$^-$ bond relations may be summarized by stating that every F$^-$ has a type I bond to two Mn^{++} and a type II bond to one Mn^{++}. The Mn^{++} axes and the surrounding fluorine distorted octahedron are indicated in Fig. 1(b).

From the relative Mn^{++}—F$^-$ positions in the unit cell it can be seen that the external magnetic field in (100) [or equivalent (010)] the two F$^-$ positions are indistinguishable and only one NMR line is to be expected, but in all other planes there will be, in general, two lines. The displacements of the lines resulting from the time-averaged local dipolar fields are calculated in Appendix A where the dipole contributions are summed over the entire crystal.

EXPERIMENTAL APPARATUS

The magnet used was a Varian Associates six-inch electromagnet. A magnetic field sweep, linear in time, was derived from a motor-driven, battery-supplied potentiometer, the voltage output of which was applied to the control grid of the magnet power supply. The field-modulation generator operated at 280 cps while the narrow-band audio-amplifier and the phase-sensitive detector were similar to those described by Watkins.[8] Two different radio-frequency units were used in the experiments. Most of the measurements were made with a Varian Associates variable-frequency induction

---

[6] M. Griffel and J. W. Stout, J. Am. Chem. Soc. **72**, 4351 (1950).

[7] M. Tinkham, Proc. Roy. Soc. (London) **A236**, 535, 549 (1956).

[8] G. D. Watkins, thesis, Harvard University, 1952 (unpublished).

spectrometer operating in the frequency range of two to sixteen Mc/sec. One measurement was made using a modified Pound-Knight-Watkins[8,9] marginal oscillator at 28 Mc/sec. Since the nuclear spin-lattice relaxation times were $\sim 10^{-6}$ second, and the line widths ~ 30 oersteds, it was necessary to use large radio-frequency fields and large modulation fields. The need for large radio-frequency fields can be appreciated by remembering that the optimum value of the radio-frequency field in an absorption experiment satisfies the condition $(\gamma H_1)^2 T_1 T_2 = 1$. If $T_1 \cong T_2 \cong 10^{-6}$ second as in our experiment, the optimum value of H_1 for the F^{19} nucleus is $1/\gamma T_2$ or ~ 30 oersteds. It was not possible to produce rf fields larger than one oersted and consequently the signal was some 30 times less than the maximum obtainable, since for H_1 smaller than the optimum value the signal is directly proportional to H_1.

The need for large rf fields emphasized the differences between the marginal oscillator and the induction spectrometer. Figure 2 is a plot of the signal-to-noise ratio measured in our marginal oscillator by using a calibrator circuit to simulate the signal. It is similar to unpublished results of Watkins and is presented to show that above a certain radio-frequency voltage across the tank circuit (in our case ~ 0.5 volt rms) the signal-to-noise ratio decreases rapidly. Since 0.5 volt rms corresponds to $H_1 \sim 0.05$ oe, the marginal oscillator was not too well suited for the $MnF_2{}^{19}$ measurement. In the induction spectrometer, on the other hand, the noise is theoretically independent of the radio-frequency level, and increasing the level to the maximum value of ~ 1 oe brought the $MnF_2{}^{19}$ resonance above the noise even at two Mc/sec. The same signal-to-noise ratio was observed at 28 Mc/sec with the marginal oscillator, although under optimum conditions the theoretical signal strength was much greater at the higher frequency.[10]

The MnF_2 single-crystal samples were grown by Dr. J. Nielsen and Mr. E. Dearborn of these Laboratories following the method described by Stout.[6] Two samples were used. Both were ground to roughly spherical shapes and were approximately 8 mm in diameter. The samples were mounted at the ends of thin-wall glass tubes with a proton-free silica cement and calibrated copper-constantan thermocouples were embedded in the cement. One sample had its [001] direction along the tube axis allowing the external magnetic field, H_0, upon rotation, to take any direction in the (001) or *ab* plane. Similarly, the other sample was oriented with the [110] direction parallel to the tube axis. The choice of these two orthogonal planes enabled the external field to be directed along all of the important crystalline axes. Samples were placed in the tip of an unsilvered glass Dewar whose outside and inside diameters were 1.5 cm and 1.0 cm, respectively. Although fixed temperatures like the boiling points of nitrogen and oxygen were easily maintained, intermediate temperatures were unstable because of the rapid heat losses and lack of heat transfer between the main body of coolant and the tip of the Dewar. The filling factor was ~ 0.05 for both samples.

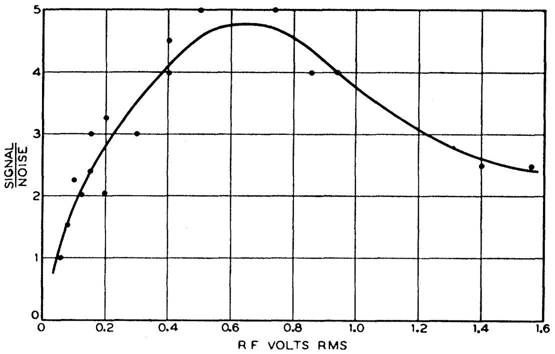

FIG. 2. Ratio of signal-to-noise in oscillator-detector as a function of voltage across tank circuit.

EXPERIMENTAL RESULTS

When H_0 lies in the (100) or (010) plane, only one F^{19} resonance line will be observed. When H_0 is not in this plane two lines are expected although they may not always be resolved. The first group of experiments which we shall discuss consisted of orienting the MnF_2 crystal so that H_0 was parallel to the [001] direction and measuring the shift of the single F^{19} resonance as a function of temperature and of H_0. The *c* axis, [001], was chosen because of its particular importance in the antiferromagnetic state. All of the data presented in the text have been corrected for the internal fields calculated from the dipole sum and also include a demagnetizing correction of $4\pi M/3$ appropriate to our spherical samples. For example at room temperature, and 1000 oe, where $4\pi M/3 \cong 2$ oe the demagnetizing factor is almost negligible compared to the line width (which determines accuracy of measurements), but it is appreciable at 77°K and 3800 oersteds where $4\pi M/3 = 16.8$ oe. However, the data shown in the figures are uncorrected and in general will not agree with the values quoted in the text. The shift of the resonance from the normal resonance field of ω/γ is defined as ΔH. Figure 3 is a plot of ΔH *vs* H_0 at 77°K. It can be seen that ΔH is proportional to H_0 and can be represented by the relation $\Delta H = (0.0735 \pm 0.0003) H_0$ when the above-mentioned corrections are applied. This shift is orders of magnitude larger than the small shifts observed in nuclear resonances in diamagnetic materials. Since the dipole sum and the demagnetization

---

[9] R. V. Pound and W. D. Knight, Rev. Sci. Instr. 21, 219 (1950).

[10] The primary source of 280-cps noise in the marginal oscillator is the oscillator tube itself. Operating in a nonlinear range it mixes its own flicker and shot noise with the rf, resulting in a low-frequency amplitude modulation of the rf carrier. To the extent that the first tube in the rf receiver is responsible for the noise in the induction spectrometer it is operating in a linear region, not mixing in its own noise, and consequently independent of H_1, provided the imbalance is maintained at a constant level.

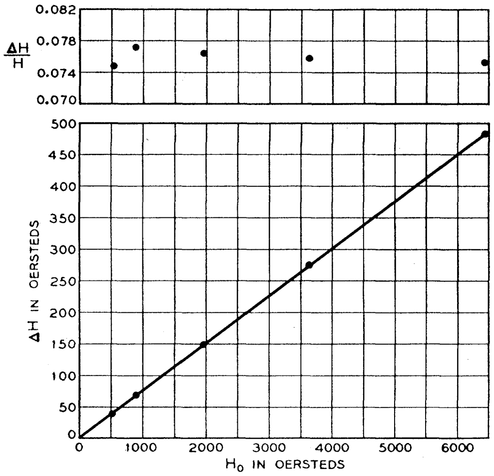

FIG. 3. Plot of ΔH *vs* H_0 for $H_0 \| [001]$, where $\Delta H = (\omega/\gamma_N) - H_0$. The upper curve is a plot of the fractional field displacement, $\Delta H/H_0$.

fields have been considered as corrections on the measurements clearly some other mechanism must be found to explain these large shifts.

The shift ΔH has also been measured as a function of temperature for H_0 along [001]. In Fig. 4 we have plotted ΔH *vs* temperature. Here we plot the temperature dependence of the magnetic susceptibility[11] parallel[12] to [001] on the same graph, arbitrarily taking the ordinates to be the same at one temperature (77°K). We see that ΔH is proportional to the susceptibility within the experimental errors of both measurements for temperatures below room temperature but the shift does not agree with the susceptibility at 300°K. The data presented in Fig. 4 are uncorrected but both corrections are proportional to H_0 and should not cause any deviations from the normalized susceptibility. Since the dependence of the shift upon the susceptibility is, we feel, very well established we can only conclude that the susceptibility data has larger errors than have been indicated.

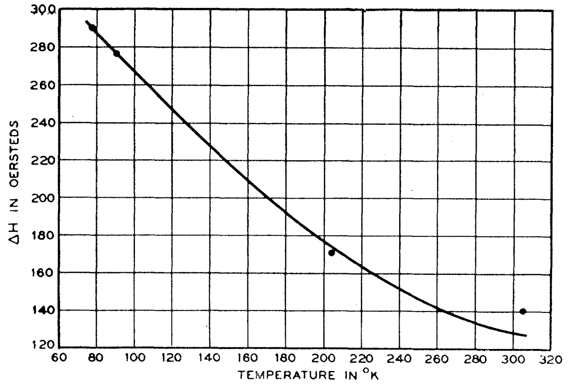

FIG. 4. Plot of ΔH *vs* absolute temperature for $H_0 \| [001]$. The solid curve is magnetic susceptibility parallel to [001], $\chi_{\|}$, normalized to fit experimental value of ΔH at 77°K.

At 77°K and $H_0 \sim 3700$ oersteds the two separate F^{19} lines could be resolved and their angular dependence measured. The observed angular dependence of the separate lines is similar to that expected from the dipole sum fields as shown in Appendix A. Figure 5 shows the positions of the resolved doublet for H_0 in the *ab* plane as a function of the angle φ between H_0 and [110]. The first point to be made about the observed splittings is that the center of the pattern, corresponding to the single line observed when $\varphi = 0°$, is displaced by $\Delta H = (0.0734 \pm 0.0005) H_0$ when corrected. Secondly, as would be expected from the symmetry of the F^{19} sites in the crystal, the splitting observed has fourfold symmetry about [001].

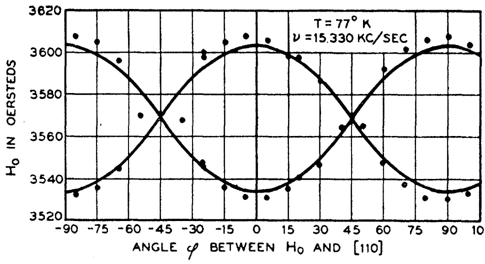

FIG. 5. Fields for resonance for resolved lines *vs* φ, where H_0 is in the (001) plane and φ is the angle between H_0 and [110]. The solid curve shows the anisotropy expected from the dipole sum. It has been displaced from its true position so as to coincide with the measured values at $\varphi = \pm 45°$. The residual anisotropy is caused by the electron transfer. (Note comment in Table I caption concerning uncertainty in dipole sum correction.)

The solid line represents the anisotropy calculated from the dipole sum. This curve has been drawn to show how the anisotropy of the dipole sum almost fits the anisotropy of the splitting (numerical values are given below). However, the dipole sum does not explain the isotropic shift of 7.34% mentioned above. Consequently the solid curve has been drawn displaced by 262 oersteds from its predicted position.

The singlet observed with H_0 along [100] is at the mean position of the pattern found in the (001) plane. It will be shown below that this is to be expected. However, the single line for $H_0 \| [001]$ might be at any position with respect to the (001) pattern. We present in Fig. 6 the splittings observed when H_0 is rotated through different positions in the (110) plane. There is only twofold symmetry about [110]. The single line observed with $H_0 \| [001]$, as we shall see, is not to be expected at the mean of the maximum splitting in the (001) plane although, again, the asymmetry observed is very close to that predicted by the dipole sum.

---

[11] H. Bizette and B. Tsai, Compt. rend. **209**, 205 (1939); deHaas, Schultz, and Koolhaas, Physica **7**, 57 (1940). In the solid curve of Fig. 4 we have plotted the latter's values. More recent measurements in a more limited temperature range by Corliss, Delabarre, and Elliott, J. Chem. Phys. **18**, 1256 (1950) indicate different values of the susceptibility above 200°K.

[12] M. Griffel and J. W. Stout, J. Chem. Phys. **18**, 1455 (1950).

LINES SHAPES AND WIDTHS

A typical recorder trace of the unresolved fluorine resonance with $H_0\|[001]$ at 77°K is presented in Fig. 7. It can be seen that the observed line is close to Lorentian in shape. Furthermore the individual lines, when resolved, were also Lorentzian. The separations between the extreme values of the absorption derivatives, which we shall call the line widths and designate by δH, were measured as a function of temperature with $H_0\|[001]$ for $\gamma = 15.666$ Mc/sec. The line widths were independent of the strength of the radio-frequency field, H_1, and the intensities were directly proportional to H_1. These observations, considered in conjunction with the Lorentzian shape, led to the conclusion that the lines were exchanged-narrowed with $T_2 = (\frac{1}{2}\sqrt{3}\gamma\delta H)^{-1}$. A detailed correlation between experiment and theory is given in a later section.

ANTIFERROMAGNETIC TRANSITION

In order to observe the behavior of the F^{19} resonance at the antiferromagnetic transition temperature the resonance was displayed on an oscilloscope. The oscilloscope was swept synchronously with the magnetic field at 0.2 cps. The amplitude of the field sweep was ~200 oersteds. The signal-to-noise ratio was maintained at about 5:1 by presenting the undetected output of the narrow-band (15-cps band width) 280-cps amplifier on the oscilloscope. No very rapid changes in the resonance fields were observed as the temperature was lowered from 77°K to 68°K. At 68±1°K and with a temperature variation across the sample of <0.5°K, the resonance was seen to disappear without first broadening or shifting its position. Since this is the antiferromagnetic transition[13] temperature region, we associate this behavior with the onset of long-range order. This will be discussed more fully in the following section.

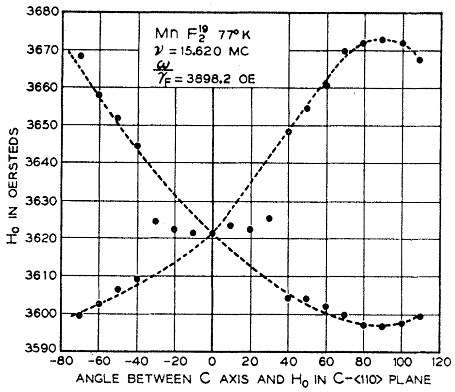

FIG. 6. Fields for resonance for resolved lines *vs* ψ, where H_0 is in the (110) plane and ψ is the angle between H_0 and [001]. The lines were not resolved for $\psi \sim 0°$.

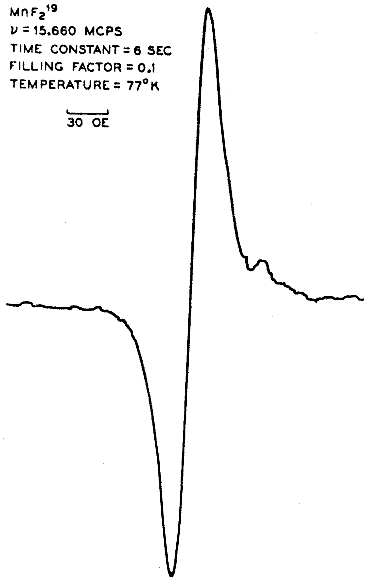

FIG. 7. Recorder trace of derivative of unresolved line with $H_0\|[001]$ and $T = 77$°K.

INTERPRETATION

The most striking experimental results to be explained are the large shifts of the fluorine resonance. These shifts have the same temperature and field dependence as the bulk magnetization. In addition the anisotropy of the two fluorine resonances must be compared with that predicted from magnetic dipole interactions alone. To the extent that experimental conditions allow the lines to be resolved, the anisotropy appears to be proportional to the magnetization. After discussing these effects, we shall go on to consider the line widths and the behavior of the resonances in the vicinity of the antiferromagnetic transition.

The explanation of the above phenomena can be found in the fact that large fields exist at the fluorine nuclei because the $Mn^{++}-F^-$ bond is not purely ionic. The covalent bond to the paramagnetic ion requires that the electron transferred from the F^- to Mn^{++} has its spin opposite to that of the Mn^{++}. The unpaired electron remaining on the F^- ion, with spin parallel to that of the paramagnetic ion, produces its characteristic hyperfine field at the F^{19} nucleus. This may be paraphrased by saying that since all spins are paired on the F^- ion the electron in the antibonding orbital has the same spin orientation as the Mn^{++} electrons. These ideas may be formalized in a manner which quantitatively yields the percentage of covalent bonding, the angular dependence of the bonds and the dependence of the interaction on the local magnetization at a Mn^{++} site.

Following our brief, initial report[14] of this investigation Bleaney[15] showed that the NMR measurements

---

[13] J. W. Stout and H. E. Adams, J. Am. Chem. Soc. **64**, 1535 (1942), report 66.5°K as the heat-capacity maximum.

[14] R. G. Shulman and V. Jaccarino, Phys. Rev. **103**, 1126 (1956).

[15] B. Bleaney, Phys. Rev. **104**, 1190 (1956).

in MnF_2 complement, and can be correlated with, the paramagnetic resonance studies by Tinkham[7] of Mn^{++} as a dilute substitutional impurity in the isomorphic diamagnetic crystal ZnF_2. Tinkham had observed that each of the hfs lines of the Mn^{++} paramagnetic resonance could be resolved into components. This additional hfs he explained by considering a certain amount of covalency to exist between each Mn^{++} and the six surrounding F^- ions. A detailed comparison between our findings and Tinkham's is presented in Appendix B.

To consider the effects of an electron-nuclear interaction on the energy levels of a nuclear magnetic moment in an external field we construct[16,17] the following nuclear Hamiltonian, in component form

$$\mathcal{H}_0 = -\gamma_N\hbar \sum_{i=1}^{3} I_i H_i + \sum_{j=1}^{3}\sum_{i=1}^{3} A_i{}^j I_i \langle S_i\rangle^j, \tag{1}$$

where the jth sum extends over the three nearest Mn^{++} neighbors of each F^- and $\langle S_i\rangle^j$ is the thermal average of S in the ith direction on the jth Mn^{++} and where i runs over x, y, and z. The principal values of A along the x, y, and z directions we designate by A_1, A_2, and A_3, respectively. We assume that the principal axes of the hyperfine interaction and magnetocrystalline anisotropy tensors coincide (the surface of the latter is an ellipsoid of revolution about the c axis in the case of MnF_2). If ζ is the direction of the resultant field at the nucleus, an orthogonal transformation of the coordinate system must be made to diagonalize $\mathcal{H}_0$, so that $\mathcal{H}_0 = -\hbar\omega_0 I_\zeta$, where the resonant frequency is given by

$$\omega_0 = \gamma_N \left[\sum_i \left(H_i - \sum_j \frac{A_i{}^j}{\gamma_N\hbar}\langle S_i\rangle^j\right)^2\right]^{\frac{1}{2}}. \tag{2}$$

Thus, except for the special cases of the field along a principal axis, either magnetic anisotropy or an anisotropic hyperfine interaction will insure that the direction of nuclear quantization and the external field do not coincide. If there is no magnetic anisotropy (approximately the case for MnF_2 in the paramagnetic state) then $\langle S_i\rangle = \text{constant}\times H_i$ and the thermal average may be calculated in the high-temperature limit, or more directly, related to the measured susceptibility as is done in Appendix A. In this way Eq. (2) may be expressed as

$$\omega_0{}^a = \gamma_N\Big[\sum_i H_i{}^2\big(1+\alpha\sum_j A_i{}^{ja}\big)^2\Big], \text{ where } \alpha = \frac{\chi}{Ng\beta\gamma_N\hbar}, \tag{3}$$

with a corresponding expression for $\omega_0{}^b$, and where the superscripts a and b refer to the fact that there are two resonant frequencies to be expected, in general, corresponding to the two nonequivalent F^- sites in a unit cell. [The sign change in Eq. (3) occurs as a result of the electron spin momentum being opposite to that of its magnetic moment.] If there is magnetic anisotropy, Eq. (3) would be correct only for H_0 parallel to one of the principal axes. It can easily be shown that our Eq. (3) reduces to Bleaney's[15] Eq. (2), except for his incorrect sign, for $\alpha A_i \ll 1$, but that when H_0 is not parallel to a principal direction his expression is only a first approximation.

The choice of x, y, and z directions in the crystal are shown in Fig. 1(b). Because of the 90° rotation about the z axis in going from one Mn^{++} site to the next in the unit cell, the x and y directions for one Mn^{++} will be the y and x of the other. The components of A along the principal axes are, for the two fluorine resonances,

	Line a	Line b
A_1	$2A_x{}^{I}+A_y{}^{II}$	$2A_y{}^{I}+A_x{}^{II}$
A_2	$2A_y{}^{I}+A_x{}^{II}$	$2A_x{}^{I}+A_y{}^{II}$
A_3	$2A_z{}^{I}+A_z{}^{II}$	$2A_z{}^{I}+A_z{}^{II}$

Thus, for example, in the approximation αA_1 and $\alpha A_2 \ll 1$ the angular dependence of the fractional shift of the resonant field for the two lines in (001) is

$$\begin{aligned}(\Delta H/H_0)_a &= \alpha[(2A_y{}^{I}+A_x{}^{II})\cos^2\varphi \\ &\qquad + (2A_x{}^{I}+A_y{}^{II})\sin^2\varphi],\\ \text{and} \\ (\Delta H/H_0)_b &= \alpha[(2A_x{}^{I}+A_y{}^{II})\cos^2\varphi \\ &\qquad + (2A_y{}^{I}+A_x{}^{II})\sin^2\varphi],\end{aligned} \tag{4}$$

where φ is the angle between [110] and H_0. The maximum fractional error in this approximation is of the order of the fractional field shift. At $\varphi = \pm 45°$, corresponding to [010] or [100], both lines coincide at $[A_y{}^{I}+A_x{}^{I}+\frac{1}{2}(A_y{}^{II}+A_x{}^{II})]$ which is also the mean shift of the two lines for all values of φ. At $\varphi = 0$ the two lines are displaced by $(2A_y{}^{I}+A_x{}^{II})$ and $(2A_x{}^{I}+A_y{}^{II})$. It will be shown below how we can distinguish between these two lines on theoretical grounds and decide that $(2A_y{}^{I}+A_x{}^{II}) > (2A_x{}^{I}+A_y{}^{II})$. With this inequality we are able to determine experimentally two combinations of the A's from the measurements with H_0 in (001). The third and last independent measurement possible by NMR is made with $H_0 \| [001]$. In Fig. 6 these results are displayed ($\psi = 0°$) along with the [110] splittings. The mean of these splittings, as mentioned above, is the displacement observed along the [100] direction but it is not equal to the displacement along [001] as can be seen. The approximate form of the fractional shift, for the two different fluorine positions, with H_0 in $(\bar{1}10)$, is

$$\begin{aligned}(\Delta H/H_0)_a &= \alpha[(2A_y{}^{I}+A_x{}^{II})\sin^2\psi \\ &\qquad + (2A_z{}^{I}+A_z{}^{II})\cos^2\psi],\\ (\Delta H/H_0)_b &= \alpha[(2A_x{}^{I}+A_y{}^{II})\sin^2\psi \\ &\qquad + (2A_z{}^{I}+A_z{}^{II})\cos^2\psi],\end{aligned} \tag{5}$$

---

[16] The method we adopt follows Moriya.[17] A more complete Hamiltonian is considered in Appendix A where the dipolar effects of the electron spins on the nuclear Zeeman levels are explicitly taken into account and the thermal average of S is calculated as well.

[17] T. Moriya, Progr. Theoret. Phys. Japan **16**, 641 (1956).

where ψ is the angle between H_0 and [001]. In Fig. 6 the dashed line represents the best fit between this expression including dipole-sum and electron-transfer contributions and the experimental points. The values of the hyperfine interaction determined from fitting the experimental data are listed in Table I. Tinkham's values for $\mathrm{Mn^{++}}$ in $\mathrm{ZnF_2}$ are also listed, where the direct dipolar contributions have been removed from the published values in order to allow a comparison (in Appendix B) of the hyperfine interactions alone.

It is possible[7] to write the six individual components of the hyperfine interaction in the general form

$$A_i^N = A_s^N + A_\sigma^N(3\cos^2\theta_{i,\sigma}-1) + A_\pi^N(3\cos^2\theta_{i,\pi}-1), \tag{6}$$

where $i=x$, y, or z; $N=\mathrm{I}$ or II; A_σ^N represents the s-electron contribution which is isotropic; the anisotropic p-electron interactions come from p_σ bonds or p_π bonds represented by A_σ^N and A_π^N, and $\theta_{i,\sigma}$ and $\theta_{i,\pi}$ describe the angles between the ith direction and the directional p_σ and p_π bonds, respectively. In this general form we have expressed the A's as functions of six unknowns by indicating that the s, p_σ, and p_π components of type I bonds may be different from those of type II bonds. Since we measure only three independent parameters we chose to disregard the differences between the two types of bonds following the reasons given in Appendix B. Assuming this, and substituting numerical values for the $\mathrm{MnF_2}$ lattice, we have

$$\begin{aligned} A_x^{\mathrm{I}} &= A_s - A_\sigma + 2A_\pi, & A_x^{\mathrm{II}} &= A_s + 2A_\sigma - A_\pi, \\ A_y^{\mathrm{I}} &= A_s + 0.19A_\sigma - A_\pi, & A_y^{\mathrm{II}} &= A_s - A_\sigma + 2A_\pi, \\ A_z^{\mathrm{I}} &= A_s + 0.81A_\sigma - A_\pi, & A_z^{\mathrm{II}} &= A_s - A_\sigma - A_\pi. \end{aligned} \tag{7}$$

Rewriting these expressions in the form required for comparison with the experimental measurements, we have

$$\begin{aligned} 2A_z^{\mathrm{I}} + A_z^{\mathrm{II}} &= 3A_s + 0.62A_\sigma - 3A_\pi, \\ 2A_y^{\mathrm{I}} + A_x^{\mathrm{II}} &= 3A_s + 2.38A_\sigma - 3A_\pi, \\ 2A_x^{\mathrm{I}} + A_y^{\mathrm{II}} &= 3A_s - 3.0A_\sigma + 6A_\pi. \end{aligned} \tag{8}$$

Since the σ contributions should be larger than the π and since upon solving these equations we find $A_\sigma > A_\pi$, the justification for considering $(2A_y^{\mathrm{I}}+A_x^{\mathrm{II}}) > (2A_x^{\mathrm{I}}+A_y^{\mathrm{II}})$ is now clear. The other alternative leads to impossible negative values of A_σ in the case of $\mathrm{Mn^{++}}$. The values of the individual components converted to energy units are $A_s = (15.7\pm0.3)\times10^{-4}\ \mathrm{cm^{-1}}$, $A_\sigma = (0.6\pm0.3)\times10^{-4}\ \mathrm{cm^{-1}}$, and $A_\pi = (0.2\pm0.3)\times10^{-4}\ \mathrm{cm^{-1}}$.

TABLE I. Experimentally determined values of hyperfine interaction in $\mathrm{MnF_2}$ and $\mathrm{Mn^{++}}$ in $\mathrm{ZnF_2}$ (reference 7). The limits of error in the NMR values are of experimental origin and do not include uncertainties arising from the point-dipole assumption in applying the dipole sum correction. Tinkham's values of the hyperfine interaction constants have been corrected by subtracting the $\mathrm{F^{19}}$ dipolar contribution from the values given in reference 7.

$\mathrm{MnF_2}(10^4\ \mathrm{cm^{-1}})$	$\mathrm{ZnF_2{:}Mn^{++}}(10^4\ \mathrm{cm^{-1}})$
$2A_z^{\mathrm{I}}+A_z^{\mathrm{II}}=47.0\pm0.5$	$A_z^{\mathrm{I}}=17.0\pm0.2$
$2A_y^{\mathrm{I}}+A_x^{\mathrm{II}}=47.8\pm0.5$	$A_z^{\mathrm{II}}=13.9\pm0.2$
$2A_x^{\mathrm{I}}+A_y^{\mathrm{II}}=46.3\pm0.5$	$A_y^{\mathrm{I}}=16.3\pm0.7$
	$A_y^{\mathrm{II}}=16.0\pm1.3$

With these values for the A's, the percentage of fluorine s and p unpaired electrons may be determined. We consider the fluorine bonding electrons to be $2s$ and $2p$ for the reasons given in Appendix B. The hyperfine interactions[5] of these electrons are, in $\mathrm{F^-}$,

$$\begin{aligned} A_{2s} &= (8/3)\pi g\beta\gamma_N\hbar|\psi(0)|_{2s}^2 = 1.57\ \mathrm{cm^{-1}}, \\ A_{2p} &= \tfrac{2}{5}g\beta\gamma_N\hbar\langle 1/r^3\rangle_{2p} = 0.044\ \mathrm{cm^{-1}}, \end{aligned} \tag{9}$$

respectively, where $|\psi(0)|_{2s}^2$ is the normalized probability of finding a $2s$ electron at the nucleus evaluated by Hartree[18] and $\langle 1/r^3\rangle_{2p}$ is the expectation value of $1/r^3$ for a $2p$ electron whose numerical value is given by Barnes and Smith.[19] The magnetic fields at the nucleus from these interactions are

$$\begin{aligned} H(2s) &= 6.1\times10^6\ \text{oersteds}, \\ H(2p) &= 1.8\times10^5\ \text{oersteds}. \end{aligned} \tag{10}$$

The field of the electron at the nucleus, $H_{\mathrm{h.f.}}$, may be obtained from the hyperfine interaction. By using Eq. (1), we find

$$A(\tfrac{5}{2}) = \gamma_N H_{\mathrm{h.f.}}/2\pi c, \tag{11}$$

or numerically, for fluorine, $H_{\mathrm{h.f.}} = 1.87\times10^7 A$ where A is in $\mathrm{cm^{-1}}$. From this relation it can be calculated that each fluorine-manganese bond has (0.48%±0.02%) $2s$ character. This determination of the $2s$ character and the nature of the p contributions may be seen as follows.

Let us simplify the problem by considering antibonding molecular orbitals for a diatomic $\mathrm{Mn^{++}-F^-}$ system. The functions are

$$\psi_i = N_i(\psi_{\mathrm{Mn^{++}}} - a_i\psi_{\mathrm{F^-}}), \tag{12}$$

where N_i is the normalization constant, a_i is the augmentation parameter, and $\psi_{\mathrm{F^-}}$ is a linear combination of s and p fluorine functions that are augmented, with proper symmetry, onto the $\mathrm{Mn^{++}}$ $3d$ functions. In evaluating matrix elements of the hyperfine interaction, the s-electron contact part will be proportional to a_i^2. Furthermore the coefficient of the s contribution is independent of the type of wave functions chosen to describe the bonding. On the other hand, the p character of the hyperfine interaction involves nuclear spin-electron spin and nuclear spin-electron orbital contributions from matrix elements of the form

$$\langle\bar{\psi}_i|1/r^3|\psi_i\rangle, \tag{13}$$

which will contain localized, overlap, and dipole-like contributions. These will be quite sensitive to the choice

---

[18] D. R. Hartree, Proc. Roy. Soc. (London) **151**, 96 (1935).

[19] R. G. Barnes and W. V. Smith, Phys. Rev. **93**, 95 (1954).

of wave functions. We see then that whereas the isotropic shift defines the *s* contributions to the bonding uniquely, since it is related to the contact part of the interaction, the anisotropy of the resonance shifts defines the *p* character of a bond only when specific functions are chosen.

If we adopt the Owen[20]-Tinkham type of augmented Mn^{++} molecular orbitals represented by Eq. (12), and assume that the overlap-region contributions are negligible and that only F^- $2p$ functions are admixed, we find that the $2p_\sigma$ and $2p_\pi$ character of the bond are $(0.6\pm0.3)\%$ and $(0.2\pm0.3)\%$, respectively.

In order to show what is meant by the *p* and *s* character of the bond, let us consider the bonding and antibonding functions shown in Eq. (12). Four electrons may be placed in each set of bonding and antibonding orbitals whereas only three electrons are present, namely, two from the F^- ion and one *3d* electron from the Mn^{++} ion. To the extent that a *3d* orbital with a particular spin coordinate has been mixed with fluorine orbitals in the bonding functions, the contribution of the *3d* to the antibonding orbital is reduced while the contribution of the fluorine orbitals is increased. This means that, to the extent to which bonding occurs, the unpaired electron in the antibonding orbital has the character of the fluorine functions and consequently strong hyperfine interaction with the fluorine nucleus which we measure. On the other hand, this kind of bonding of a *3d electron* will not affect the magnetic properties of the material because, to the extent to which a formerly unpaired *3d* electron is paired in the bonding orbital, a formerly paired fluorine electron is unpaired in the antibonding orbital. It is not the free-ion magnetization that is changed from the purely ionic case but rather its spatial location. We see therefore that the type of bonding which we have been discussing and which our experiments allow us to measure is different from that which has been described by Pauling[21] for the extremely covalent transition-element bond. In this latter case the maximum amount of pairing of the transition-element spins is considered to occur and the bonding orbitals of the form $4s4p^33d^2$ are occupied by electrons from the ligands. The effects of this type of bond upon the dc susceptibility have been the subject of many investigations. As Owen[20] has pointed out, the increase in energy of the antibonding $3d\gamma$ orbitals from the mixing will eventually result in a breakdown of Hund's rule of maximum spin multiplicity, thereby allowing agreement in the extremely covalent compounds between the crystalline-field and valence-bond approaches.

Since the NMR measurements determine the spatial location of the unpaired spins, they are relevant to the superexchange[22] process which ascribes long-range order to the magnetic properties of the intervening anions. The small contribution of *p* electrons to MnF_2 bonds is somewhat disquieting from the standpoint of the need of directed orbitals in the superexchange process and seems even more surprising from a bonding viewpoint. The presence or absence of *p*-electron character in the bond is associated with the corrections for the anisotropic shift of the NMR from the dipole sum. In essence we have calculated that almost all of the anisotropy can be explained by the dipole sum and have determined the $2p$ character to be small. This does not seem to be true in single-crystal FeF_2 and CoF_2 which we have measured[23] but rather it seems that an appreciable fraction of the bond will be *p*-like in character. We propose to discuss the *p* character of the bonds and the applicability to long-range order more fully in the future when more data are available on the isomorphic compounds FeF_2 and CoF_2. At the same time we shall discuss in more detail the nature of the molecular orbitals involved, the atomic functions of $n=3$ and the approximations involved in the dipole sum. However, it does not seem that the fractional *p* character will be changed appreciably by these considerations.

ANTIFERROMAGNETIC STATE

As was noted in the experimental section, the resonance was seen to disappear abruptly at T_n. Since a large discontinuous change of T_1 or T_2 is not to be expected as the NMR crosses the transition temperature, we associate the disappearance of the resonance with the fact that the abrupt rise of $\langle S\rangle$ just below T_n displaces the resonance frequency to a range outside our NMR spectrometer. The frequency dependence of the resonance in the antiferromagnetic state with H_0 parallel to [001] is

$$\nu=\frac{1}{h}(2A_z{}^{\mathrm{I}}-A_z{}^{\mathrm{II}})\frac{5}{2}\frac{M(T)}{M(0)}\pm\frac{\gamma_N}{2\pi}H_0, \tag{14}$$

since $\langle S\rangle_T$ is proportional to $M(T)$, the sublattice magnetization; we have assumed here the antiferromagnetic ordering determined by neutron-diffraction data.[24] We have neglected, in this expression, the different field dependences of the two sublattice magnetizations and the departure of the antiferromagnetic ground state from complete antiparallel alignment.

The first expression on the right-hand side gives the frequency of the fluorine resonance in the absence of an external magnetic field. From Tinkham's data Bleaney[15] has calculated this frequency to be 179 Mc/sec. By constructing $A_z{}^{\mathrm{I}}$ and $A_z{}^{\mathrm{II}}$ from our values of A_s, A_σ, and A_π, we find that this frequency should be 177 Mc/sec (where the effects of the dipole fields, antiferromagnetically arranged, have been included). The agree-

---

[20] J. Owen, Proc. Roy. Soc. (London) **227**, 183 (1955).

[21] L. Pauling, *Nature of the Chemical Bond* (Cornell University Press, Ithaca, 1939).

[22] P. W. Anderson, Phys. Rev. **79**, 350 (1950).

[23] Jaccarino, Shulman, and Stout, Phys. Rev. **106**, 602 (1957).

[24] R. A. Erickson and C. G. Shull, Phys. Rev. **83**, 208 (1951); R. A. Erickson, thesis, Agricultural and Mechanical College of Texas, June, 1952 (unpublished).

ment is this close because our reconstructed values of A_z^{I} and A_z^{II} are close to Tinkham's. Because of the large temperature dependence of $M(T)$ just below T_n, the resonant frequency rapidly approaches the limiting value given above. In order to be able to observe the resonance at 16 Mc/sec in this temperature range, the temperature stability and homogeneity must be at least one millidegree over the sample during the time it takes to sweep through the resonance. Our temperature control was not this good and we were not able to see the resonance just below the transition temperature. In one experiment H_0 was perpendicular to [001] so that the internal and external fields would add in quadrature. No resonances were seen in this experiment either.

A preliminary attempt was made, in conjunction with Dr. A. L. Schawlow, to observe the resonance at 4°K, 20°K, and 45°K using a frequency-swept, frequency-modulated superregenerative detector.[25] Experimental conditions were somewhat unfavorable (extremely small filling factor), and in the range of frequencies 90 Mc/sec to 250 Mc/sec (with varying sensitivity at any given frequency) no resonance was to be found.*

T_1 AND T_2 FOR THE N.M.R. OF F^{19} IN MnF_2 FOR $T>T_n$

There are two mechanisms which we would expect to contribute to the line width and thermal relaxation of the F^{19} nuclei in MnF_2: first, considerable dipolar broadening from the fluctuating paramagnetic ions and, second, the intense hyperfine field resulting from electron transfer. The relative importances of each may be estimated from an order of magnitude calculation. The dipolar field is of order

$$H_d \sim 2(g\beta\bar{S}/a^3) \sim 1.3\times 10^4 \text{ oe},$$

where a is the nearest $F^{-}-Mn^{++}$ distance, while the hyperfine field $H_{\mathrm{h.f.}}$ is of order

$$H_{\mathrm{h.f.}} \sim (2A^{\mathrm{I}}+A^{\mathrm{II}})/\hbar\gamma_N \sim 9\times 10^4 \text{ oe}.$$

Since in MnF_2 the virtual exchange field $H_e \gg H_d$ or $H_{\mathrm{h.f.}}$, we may expect appreciable exchange narrowing with both $1/T_1$ and $1/T_2$ to be of order $\gamma_N(H_d^2/H_e)$ and $\gamma_N(H_{\mathrm{h.f.}}^2/H_e)$, respectively, for the two postulated mechanisms. It is clear that the hyperfine interaction is at least an order of magnitude more important in the consideration of the relaxation times.

Recently Van Kranendonk and Bloom[4] as well as Moriya[5] have independently calculated the relaxation times expected for nuclei of nonmagnetic ions in antiferromagnetic substances. The relaxation fields were considered to be dipolar in origin. Moriya has subsequently[17] considered the relaxation of nuclei of magnetic ions in antiferromagnetic substances both in the paramagnetic state and in the antiferromagnetic state where the primary mechanism is the relaxation due to the hyperfine interaction (e.g., Mn^{55} in MnF_2). Our order-of-magnitude estimate shows that Moriya's latter calculation (with slight modification) is the one appropriate to F^{19} in MnF_2 rather than the aforementioned dipole calculations. Indeed, on the basis of dipolar relaxation alone both authors were unable to explain the original unsuccessful attempt of Bloembergen and Poulis[1] to see the MnF_2^{19} resonance. Moriya, in his first paper,[5] unaware of our original note,[14] suggested that electron transfer or superexchange must be operative in this case.

Moriya's theory may be applied to F^{19} in MnF_2 as follows. Let us assume that the principal axes of the hyperfine interaction and magnetocrystalline anisotropy tensors coincide. We designate the principal values of $A_{\mathrm{h.f.}}$ by A_1, A_2, and A_3, respectively. [The A_i's to be used are not the corrected values given in the previous section but include the dipolar contributions, at least those from the three nearest Mn^{++} neighbors (these three, by the way, account for 90% of the total dipolar field). We would like to point out that the dipolar and the p-like contributions to the hyperfine interaction are indistinguishable.] The total Hamiltonian is

$$\mathcal{H}=\mathcal{H}_0+\mathcal{H}_e+\mathcal{H}', \tag{15}$$

where $\mathcal{H}_0$ is the nuclear Zeeman term given in Eq. (1), $\mathcal{H}_e$ includes all the electron-spin interactions of which the exchange terms are most important in our problem, and

$$\mathcal{H}'=\sum_{i=1}^{3} A_i I_i(\delta S_i)$$

is the time-dependent perturbation. The spin fluctuation $\delta\mathbf{S}$ is related to the thermal average of $\mathbf{S}$, $\langle\mathbf{S}\rangle$ by

$$\delta\mathbf{S}=\mathbf{S}-\langle\mathbf{S}\rangle. \tag{16}$$

As we noted before, when H_0 and ζ are parallel then $\langle S_\zeta\rangle=\text{constant}\times\chi$ and $\langle S_\perp\rangle=0$. However, the spin fluctuations δS in the paramagnetic state are large ($\delta S \simeq S$) and essentially isotropic. When $\mathcal{H}_0$ is diagonalized, the perturbing Hamiltonian $\mathcal{H}'$ may be written as

$$\mathcal{H}'=I_\zeta V_\zeta+\tfrac{1}{2}(I_+V_-+I_-V_+), \tag{17}$$

where for example the "adiabatic" component

$$I_\zeta V_\zeta=I_\zeta\sum_{i=1}^{3}\cos\theta_i A_i(\delta S_i),$$

and $\cos\theta_i$ is the direction cosine between ζ and the ith principal axes.

Thus the adiabatic and nonadiabatic components of

---

[25] A. L. Schawlow, J. Chem. Phys. 22, 1211 (1954).

* *Note added in proof.*—The high-frequency NMR in the antiferromagnetic state has subsequently been observed by the authors; see U. Jaccarino and R. G. Shulman, Phys. Rev. 107, 1196 (1957).

H' will each involve all of the components of the spin fluctuations.[26,27]

By using this formalism, expressions for $1/T_2$ and $1/T_1$ may be derived which can be written as follows:

$$1/T_2=K\left[\sum_{i=1}^{3}(\cos^2\theta_i+\tfrac{1}{2}\sin^2\theta_i)A_i^2\right],$$
$$1/T_1=K\sum_{i=1}^{3}\sin^2\theta_i A_i^2, \tag{18}$$

where

$$K=(\pi/2)^{\frac{1}{2}}\frac{S(S+1)}{3\hbar^2\omega_e}$$

in which the angular dependence of the secular and nonsecular contributions to the line width are clearly revealed.

Only in the case in which the hyperfine interaction is isotropic will $T_1=T_2$. Physically this would be expected if both the electron-spin fluctuations and the electron-nuclear coupling is isotropic. When the electron-spin fluctuations are anisotropic—as is the case in the antiferromagnetic state—then the isotropy of the hyperfine interaction will still not make $T_1=T_2$.

To correlate the experimental line widths with the above theory we must relate the separate lines to their hfs components which are given in the previous section but uncorrected for the dipolar contributions. This formulation must be consistent with the fact that in those field directions in which only one line is observed $1/T_2^a\equiv 1/T_2^b$, where now

$$1/T_2^a=K\sum_{i=1}^{3}(\cos^2\theta_i+\tfrac{1}{2}\sin^2\theta_i)(A_i^a)^2,$$
$$1/T_2^b=K\sum_{i=1}^{3}(\cos^2\theta_i+\tfrac{1}{2}\sin^2\theta_2)(A_i^b)^2. \tag{19}$$

For $H_0\|[001]$, the theoretical and experimental line widths may be compared at high temperatures. In Fig. 8 the experimental values of δH are seen to approach 43 oe at T_∞, which corresponds to $1/T_{2\infty}=0.94\times10^6$ sec^{-1} [using the relation for Lorentzian lines of $1/T_2=(\sqrt{3}/2)\gamma\delta H$]. We have calculated ω_e from the relation

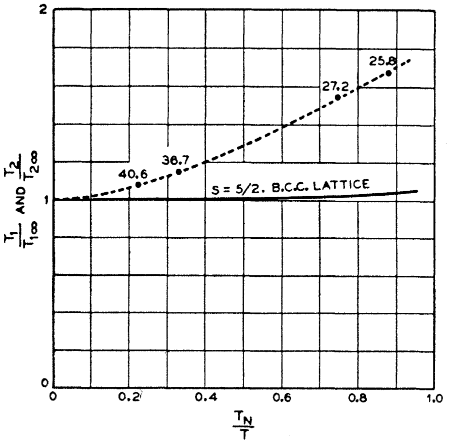

FIG. 8. A plot of the normalized theoretical nuclear spin-lattice relaxation time $T_1/T_{1\infty}$ *vs* the reciprocal of the reduced temperature, T_n/T, for a b.c.c. lattice with $S=\frac{5}{2}$ is given in the solid curve. The dotted curve gives the normalized experimental reciprocal line width, $T_2/T_{2\infty}$ *vs* the reciprocal of the reduced temperature. The numbers over the points on this curve are the measured line widths in oersteds.

---

[26] Moriya used the Kubo-Tomita (K-T) formalism[27] in which the line contour is obtained as the Fourier transform of the electron-spin correlation function. The latter is constructed from the time-dependence of the components of the density matrix of the perturbing hyperfine-structure interaction

$$I(\omega)=\int_{-\infty}^{\infty}e^{i\omega t}-\psi(t)dt,$$

where

$$\psi(t)=\int_0^t(t-\tau)\langle V_\zeta(\tau)V_\zeta(0)\rangle d\tau+\int_0^t(t-\tau)\langle V_\pm(\tau)V_\mp(0)\rangle d\tau,$$

where for example

$$\langle V_\zeta(\tau)V_\zeta(0)\rangle =\mathrm{Tr}\{\exp(-\beta\mathcal{H}_e)\tfrac{1}{2}[e^{\Gamma}V_\zeta e^{-\Gamma}V_\zeta+V_\zeta e^{\Gamma}V_\zeta e^{-\Gamma}]\}/\mathrm{Tr}[\exp(-\beta\mathcal{H}_e)];$$

here $\beta=1/kT$, and $\Gamma=i\hbar^{-1}\tau\mathcal{H}_e$.

In general a perturbation expansion is made of the elements of the density matrix. For the high-temperature region, where the electron-spin fluctuation spectrum is unknown, Anderson's[2] model of Gaussian random-frequency modulation can be used to calculate the correlation functions. (The $O_\pm O_\mp$ symbol is used for the symmetrized "raising" and "lowering" operator products.)

The adiabatic functions $\langle V_\zeta(t)V_\zeta(0)\rangle$ correspond to the time-dependent components of the hyperfine interaction that are along the direction ζ of nuclear quantization, whereas the non-adiabatic functions $\langle V_\pm(t)V_\mp(0)\rangle$ are the transverse components.

Now if the respective correlation functions decay in times τ_ζ and $\tau_\pm$ which are small compared to $1/\omega_0$ (which will be rigorously true for the case of exchange narrowing considered here), it can be readily shown that $\psi(t)$ approaches

$$\psi(t)=|t|\left[\int_0^\infty\langle V_\zeta(\tau)V_\zeta(0)\rangle d\tau+\int_0^\infty\langle V_\pm(\tau)V_\mp(0)\rangle d\tau\right]$$

the Fourier transform of which leads to a Lorentzian line shape. The frequency half-width of the line is then defined as $1/T_2$, where $1/T_2=1/T_2'+1/T_1'$ and $1/T_2'=\int_0^\infty\langle V_\zeta(\tau)V_\zeta(0)\rangle d\tau$, $1/T_1'=\int_0^\infty\langle V_\pm(\tau)V_\mp(0)\rangle d\tau$ are the contributions to the line width arising from the secular and nonsecular parts of the perturbing Hamiltonian respectively. The nonsecular part $1/T_1'$ contributes appreciably if the decay time $\tau_\pm$ of the associated "transverse" correlation function is short compared with $1/\omega_0$ and therefore assists in "lifetime" broadening of the line.

The reciprocal of the thermal relaxation time, T_1, of the nuclei is given explicitly in the K-T theory as the Fourier component of the "transverse" correlation function at the resonant frequency ω_0:

$$\frac{1}{T_1}=\int_{-\infty}^{\infty}\cos\omega_0 t\langle V_\pm(t)V_\mp(0)\rangle dt.$$

In the case of extreme narrowing, where $\omega_0\tau_\pm\ll1$, the transverse correlation function is appreciably different from zero only for $t\lesssim\tau_\pm$ and $\cos\omega_0 t$ is thereby nearly unity so that

$$\frac{1}{T_1}=\int_0^\infty\langle V_\pm(t)V_\mp(0)\rangle dt.$$

(we have used the fact that the correlation function is an even function). Thus, $1/T_1$ is just twice the nonsecular contribution to the line width.

For temperatures such that $kT\gg J$, the components of the electron-spin correlation functions, using the Gaussian assumption for the local field spectra, are given by[2]

$$\langle S_z(t)S_z(0)\rangle=\tfrac{1}{2}\langle S_\pm(t)S_\mp(0)\rangle=\tfrac{1}{3}S(S+1)\exp(-\tfrac{1}{2}\omega_e{}^2t^2),$$

where ω_e is the exchange frequency.

[27] R. Kubo and K. Tomita, J. Phys. Soc. Japan **9**, 888 (1954).

$\omega_e = g\beta H_e$. By combining Keffer's[28] estimate of 9000 oe for the magnetic anisotropy field, H_a, with the extrapolated value of $(2H_aH_e)^{\frac{1}{2}}$ obtained from recent antiferromagnetic-resonance measurements[29] of 9×10^4 oe, we obtain the value of $\omega_e = 7\times10^{12}$. Using this value in Eq. (19), we find that $1/T_{2\infty} = 0.95\times10^6$ sec^{-1}. The close agreement between these values must be fortuitous because of the uncertainty in ω_e.

In his first paper[5] Moriya calculated the temperature dependence of the electron-spin correlation functions by making a series expansion of the correlation function (following K-T) and then evaluated each coefficient in the series by a power-series expansion in $1/kT$. The temperature dependence of $T_1/T_{1\infty}$, in terms of the reduced temperature T_n/T, for the case of $S=\frac{5}{2}$ and a body-centered cubic lattice as given in reference 5, is replotted in Fig. 8. We have, as well, plotted our experimental measurements of the temperature dependence of $T_2/T_{2\infty}$ for $H_0 \| [001]$, where $T_{2\infty} \simeq T_{1\infty}$ is the calculated value given above. We have assumed that the temperature dependence, in the paramagnetic region, for the relaxation times is essentially identical for both the dipolar and hf broadening mechanisms since in either case the "narrowing" is linearly dependent on the electron-spin correlation time. Since, for $T > T_n$, $(T_2)_T \simeq (T_1)_T$, it is clear that the theory is less than adequate to account for the effects of short-range order on the local field spectra. It is interesting to note that Bloembergen and Poulis[1] stated that the reason they had not seen the $MnF_2{}^{19}$ resonance was probably that T_1 was too short. They estimated that $T_1 < 10^{-6}$ second would explain the resonance not being visible with their equipment. This agrees well with our measured values.

To make a proper comparison of the predicted anisotropy in the line width, in view of the apparent incorrectness of the predicted temperature dependence as T approaches T_n, the anisotropy should have been measured at high temperatures. Unfortunately the experimental conditions were such that at $T = 300$°K the splitting is of the order of the line widths or less, and only at 77°K might one consider the lines to be resolved. If we assume the temperature dependence of line widths to be isotropic, then we may define a line-width anisotropy factor as follows[30,31]:

$$\mathfrak{A}(1/T_{2\infty})_{\mathrm{th}} \equiv \frac{(1/T_2{}^a - 1/T_2{}^b)_{110}}{(1/T_2{}^a)_{001}} \cong \tfrac{1}{4}\left(\frac{(A_1{}^a)^2 - (A_1{}^b)^2}{(A_3{}^a)^2}\right) = 0.13, \quad (20)$$

whereas

$$\mathfrak{A}(1/T_2)_{\exp\ 77^\circ\mathrm{K}} = 0.11 \pm 0.04.$$

In Eq. (20) we see that the anisotropy in the line widths along the three principal axes is less than the anisotropy of the square of the shifts in these directions. This arises because of the sizable contributions of all three components of the hyperfine interaction to either the secular or nonsecular parts of all three line widths as shown in Eq. (19).

In CoF_2 the anistropy in the line widths is more pronounced, allowing a more detailed comparison with theory which will be reported shortly.

CONCLUSION

Large shifts and splittings of the NMR of F^{19} in MnF_2 in the paramagnetic state have been observed. The resonance was seen to disappear at the antiferromagnetic transition temperature. We have presented an explanation of the experimental observations using the theory of electron transfer and have drawn quantitative conclusion concerning the nature of the bond in MnF_2. Using Moriya's theory of nuclear relaxation processes in antiferromagnetic substances, a satisfactory explanation of the line width and the nuclear spin-lattice relaxation time at high temperatures can be given. The temperature dependence of the line width, however, is still unexplained. We believe these experiments point out the importance of NMR studies of nuclei of *nonmagnetic* ions bound to paramagnetic ions. Information about the contributions of covalent bonding to long-range order has been obtained from these measurements.

In addition it is shown that the observation of the NMR in the ordered state would contribute to our understanding of antiferromagnetism (spin-wave contributions to the sublattice magnetization, relaxation processes, etc.) as well as determine one more independent parameter of the bonding. Preliminary unsuccessful attempts to observe the NMR in the ordered state are described. In addition to the shifts observed in compounds reported in reference 23, we have also observed shifts in AgF_2. However, the $4f$ and $5f$ electrons do not give any resonance shifts in GdF_3, NdF_3, or UF_4. A more detailed report on these compounds is in preparation.

ACKNOWLEDGMENTS

We should like to thank Dr. J. W. Nielsen, Mr. E. Dearborn, and Mr. J. L. Davis for preparing the crystals of MnF_2 used in these experiments; Dr. P. W.

---

[28] F. Keffer, Phys. Rev. **87**, 608 (1952).

[29] F. M. Johnson and A. H. Nethercot, Jr., Phys. Rev. **104**, 847 (1956).

[30] There is some indirect experimental evidence to suppose that the temperature dependence of the line widths of the NMR of F^{19} in MnF_2 may not be isotropic in the region $T_n < T \leq 3T_n$, which is the region in which the effects of short-range order are important. We have studied[31] the temperature dependence (and its anisotropy) of the paramagnetic resonance line widths of the Mn^{++} spin in MnF_2 in this same temperature range at a frequency of 50 kMc/sec. A pronounced anisotropy in the temperature dependence of the line widths exists. Qualitatively, we may suppose this is to be expected if the electron-spin correlation functions become anisotropic as short-range order sets in.

[31] V. Jaccarino (unpublished).

Anderson, Dr. A. M. Clogston, and Dr. L. R. Walker for several stimulating discussions; Mr. B. J. Wyluda for assistance in the measurements, and Dr. B. Bleaney and Dr. T. Moriya for preprints of their pertinent investigations.

We are especially indebted to Professor F. Keffer for his values of the dipole sum and Mr. H. R. Moore for the design and construction of the oscillator detector.

APPENDIX A. THE TIME-INDEPENDENT HAMILTONIAN AND THE DIPOLE SUM

A more general Hamiltonian for the kth F^{19} nucleus in a paramagnetic crystal would be, for the time-independent portion,[32]

$$\mathcal{H}_n{}^k=-\gamma\hbar\mathbf{I}_k\cdot\mathbf{H}_0+\sum_j \mathbf{I}_k\cdot\mathbf{A}_{jk}\cdot\mathbf{S}_j$$

$$+\sum_i^{(\mathrm{sh})}\gamma\hbar\mathbf{I}_k\cdot\beta\mathbf{g}\cdot\mathbf{S}\frac{(1-3\cos^2\theta_{ik})}{r_{ik}{}^3}+\mathcal{H}_{Q,S}+\mathcal{H}_{I,I}. \qquad \text{(A-1)}$$

(The last two terms represent the nuclear quadrupole interaction and nuclear spin-spin interactions. The former is absent for $I=\frac{1}{2}$ and the latter unimportant compared to the modification resulting from the second and third terms of $\mathcal{H}_n$.) The first term leads to the ordinary Zeeman energy in a diamagnetic crystal. The remaining terms are peculiar to a paramagnetic crystal.

The second term represents the hyperfine interaction resulting from covalent bonding of the F^- ion to a paramagnetic ion and has been discussed in the text.

The third term is the magnetic dipole interaction of the nuclear moment with the paramagnetic-ion moment and, as we have indicated by the superscript "sh," is shape-dependent. It is this term which describes the shift caused by the dipole sum whether in the paramagnetic or ordered states. If the sample shape is ellipsoidal, the field at equivalent nuclear sites in the unit cell will be the same and can, in principle, always be calculated if the structural constants of the crystal are known. MnF_2 is a relatively simple paramagnetic since the two ions in a unit cell are essentially identical and have an isotropic g tensor. Because of this the mean magnetization per ion, $\langle\mu_i\rangle$, can be simply related to $\langle S_i\rangle$[33]:

$$\langle\mu_i\rangle=-g\beta\langle S_i\rangle.$$

Now since the molal susceptibility is

$$\chi_m=\sum_i^N\left(-g\frac{\beta\langle S_i\rangle}{H_0}\right),$$

we may obtain $\langle S_i\rangle$ from experimental susceptibility data, i.e.,

$$\langle S_i\rangle_T=-H_0(\chi_m)_{\mathrm{exp}}/Ng\beta.$$

We wish to emphasize that in general the principal axes of the susceptibility tensor and the g tensor might not coincide and the simple relation between $\langle S\rangle$ and χ_m would not hold.

Keffer[34] has calculated the "paramagnetic shift,"

$$[\Delta H_k/H_0]_{\mathrm{P.S.}}\equiv-g\beta\langle S\rangle\textstyle\sum_i[(1-3\cos^2\theta_{ik})/r_{ik}{}^3]$$

for MnF_2 and has very kindly allowed us to use his results. This calculation is shape-independent and intentionally neglects demagnetizing effects. It would, for example, give for the dipole field of a cubic array at cubic lattice point a field of $4\pi M/3$, whereas, of course, for a sphere the true value is zero. Keffer's values for the field parallel to the indicated crystalline directions and at 77°K, are

$$\langle110\rangle,\quad 12.73\times10^{-3},\quad\text{and}\quad -6.50\times10^{-3};$$
$$[001],\quad 6.88\times10^{-3}.$$

The experimental values have been corrected in all of our calculations for the demagnetizing field $4\pi M/3$ appropriate to our spherical samples.

In the antiferromagnetic state at $T=0$°K in the absence of an external magnetic field, $\langle S_i\rangle=|S_i|$. Keffer has shown there will be a field of 12 700 oe due to the dipole sum which results in a predicted value of 177 Mc/sec including the hyperfine interaction. The application of a magnetic field parallel to [001] will remove the inversion degeneracy associated with the antiferromagnetic ordering, resulting in two lines which will diverge at a rate $\Delta\omega=2\gamma_N H_0$.

APPENDIX B

In this section we present a comparison of our data on MnF_2 with Tinkham's results on ZnF_2:Mn. In his experiments the effect of the hyperfine interaction between the Mn^{++} and the six octahedrally situated F^{19} nuclei was a further splitting of each of the hf components of the electron resonance. This occurred because the electron Larmor period is short compared to the nuclear spin-lattice relaxation time. With $I=\frac{1}{2}$ there will be 2^6 combinations of static arrays which can be reduced by symmetry to fifteen distinguishable configurations and, in the most favorable case of the z direction, Tinkham observed all fifteen lines. With the external field in other directions the lines overlapped and he was not able to determine $A_x{}^{\mathrm{I}}$ and $A_x{}^{\mathrm{II}}$. For similar reasons $A_y{}^{\mathrm{I}}$ and $A_y{}^{\mathrm{II}}$ could not be determined as accurately as could $A_z{}^{\mathrm{I}}$ and $A_z{}^{\mathrm{II}}$. His results are listed in Table I of the text.

It is possible to compare Tinkham's measured values of $2A_z{}^{\mathrm{I}}+A_z{}^{\mathrm{II}}$ with our NMR measurements of the same quantity in MnF_2. Tinkham's value for this

---

[32] We include in this the possibility of there being two or more nonequivalent nuclear positions in the unit cell as well as two or more nonequivalent paramagnetic ions and positions in the unit cell.

[33] For reasons given in the text we need only consider the thermal average of S_i, $\langle S_i\rangle$, in the time-independent nuclear Hamiltonian.

[34] F. Keffer (private communication).

quantity is $(47.9\pm0.3)\times10^{-4}$ cm^{-1} while ours is $(47.0\pm0.5)\times10^{-4}$ cm^{-1}. This close agreement between the two measurements, while slightly outside of the combined experimental errors, is quite surprising. The additional information which can be obtained from a NMR measurement on MnF$_2$, namely the resonance frequency in the antiferromagnetic state, will determine $2A_z^{\mathrm{I}}-A_z^{\mathrm{II}}$. This would allow A_z^{I} and A_z^{II} to be determined in MnF$_2$ by NMR measurements alone and would allow one to ascertain whether or not the agreement on $2A_z^{\mathrm{I}}+A_z^{\mathrm{II}}$ is accidental. Emboldened by this agreement (the percentage difference of the sums is considerably less than the percentage error in A_y^{II}), we may combine the two sets of data to determine the values of A_x^{I} and A_x^{II}. These are $A_x^{\mathrm{I}}=15.2\pm2$ and $A_x^{\mathrm{II}}=15.1\pm2$, both in units of 10^{-4} cm^{-1}. From his measurements Tinkham concluded that A_s was different in the two different type bonds and that $A_s^{\mathrm{I}}\cong1.2A_s^{\mathrm{II}}$. Since the type I bond distance is 2.04 A in ZnF$_2$ and the type II 2.05 A, Tinkham felt that this strong dependence of electron transfer upon internuclear distance was one horn of a dilemma (the other horn being the invariance of central-ion electronic properties to environment), which he resolved by considering the covalent bond to include a large fraction of fluorine 3*s* and 3*p* character. However, if we now calculate the isotropic part of our A^{I}'s and A^{II}'s by taking their sum, we find the sum of the three A^{I} components to be $(48.5\pm2.0)\times10^{-4}$ cm^{-1} and the sum of the A^{II}'s to be $(45.1\pm2.0)\times10^{-4}$ cm^{-1}. This agreement to within experimental error, while it does not contradict Tinkham's conclusions about the relative magnitudes of A_s^{I} and A_s^{II}, still, when considered in conjunction with the invariance of the hyperfine interaction with Mn^{++} environment, led us to assume, in the text, that $A_s^{\mathrm{I}}=A_s^{\mathrm{II}}$. It should be emphasized that, since the measurements reported in the text are sensitive only to sums which include $2A_s^{\mathrm{I}}+A_s^{\mathrm{II}}$ always in combination, the parameter determined as A_s in the text could be considered to be $(2A_s^{\mathrm{I}}+A_s^{\mathrm{II}})/3$. Only the NMR measurements in the antiferromagnetic state could distinguish the differences between A_s^{I} and A_s^{II}.

PHYSICAL REVIEW VOLUME 108, NUMBER 5 DECEMBER 1, 1957

Comparison of Two Procedures for Solution of Noncentric Crystal Structures Utilizing Anomalous Dispersion*

R. PEPINSKY AND Y. OKAYA
X-Ray and Crystal Structure Laboratory, Department of Physics,
The Pennsylvania State University, University Park, Pennsylvania

(Received July 26, 1957)

The two formulations of Okaya and Pepinsky for direct solution of noncentric crystal structures via anomalous dispersion are compared, and it is demonstrated that use of the $P_s(\mathbf{u})$ function is in general superior to the method in which two or more simultaneous quadratic equations are used to determine phases of individual $F_{\mathbf{h}}$ and $F_{-\mathbf{h}}$ values.

IN earlier papers we have presented two new methods for the solution of the structures and absolute configurations of noncentric crystals, utilizing the phenomenon of anomalous dispersion.[1–10] The first method involves application and interpretation of the function

$$P_s(\mathbf{u})=\textstyle\sum_{\mathbf{h}}|F_{\mathbf{h}}|^2\sin(2\pi\mathbf{h}\cdot\mathbf{u}),\qquad(1)$$

which directly provides the noncentric distribution of normal scatterers about anomalous scatterers in the asymmetric unit of the cell. The second method depends on the selection of the correct set of roots of the simultaneous quadratic equations

$$|F_{\mathbf{h}}|^2=(A_{\mathbf{h}}^{\mathrm{a.s.}}+A_{\mathbf{h}}^{\mathrm{n.s.}})^2+(B_{\mathbf{h}}^{\mathrm{a.s.}}+B_{\mathbf{h}}^{\mathrm{n.s.}})^2,\qquad(2\mathrm{a})$$

and

$$|F_{-\mathbf{h}}|^2=(A_{-\mathbf{h}}^{\mathrm{a.s.}}+A_{\mathbf{h}}^{\mathrm{n.s.}})^2+(B_{-\mathbf{h}}^{\mathrm{a.s.}}-B_{\mathbf{h}}^{\mathrm{n.s.}})^2,\qquad(2\mathrm{b})$$

where a.s. refers to the anomalous scatterers and n.s. to normal scatterers. Equations (2) can be applied if

---

* Research supported by a contract with the Office of Naval Research, and a grant from the National Institutes of Health.

[1] Okaya, Saito, and Pepinsky, Phys. Rev. **98**, 1857 (1955).

[2] Saito, Okaya, and Pepinsky, Phys. Rev. **100**, 970 (1955); Rev. Mex. Fis. **4**, 159 (1955).

[3] R. Pepinsky and Y. Okaya, Proc. Natl. Acad. Sci. U. S. **42**, 286 (1956).

[4] R. Pepinsky, Record Chem. Progr. **17**, 145 (1956).

[5] R. Pepinsky and Y. Okaya, Abstracts, American Crystallographic Association, French Lick, Indiana, Paper B-1, June, 1956 (unpublished).

[6] T. Doyne and R. Pepinsky, Abstracts, American Crystallographic Association, French Lick, Indiana, Paper B-2, June, 1956 (unpublished); see also Acta Cryst. **10**, 438 (1957).

[7] Pepinsky, Takeuchi, and Okaya, Abstracts, American Crystallographic Association, French Lick, Indiana, Paper B-4, June, 1956 (unpublished).

[8] Y. Okaya and R. Pepinsky, Phys. Rev. **103**, 1645 (1956).

[9] Pepinsky, Okaya, and Takeuchi, Abstracts, Fourth International Congress, International Union of Crystallography, Montreal, Paper 2–20, p. 28, July, 1957 [Acta Cryst. (to be published)].

[10] T. Doyne, doctoral thesis, Pennsylvania State University, 1957 (unpublished).